

Exploiting Hybrid Active and Passive Multiple Access via Slotted ALOHA-Driven Backscatter Communications

Bowen Gu, *Student Member, IEEE*, Hao Xie, *Student Member, IEEE*, Dong Li, *Senior Member, IEEE*, Ye Liu, *Member, IEEE*, Yongjun Xu, *Senior Member, IEEE*

Abstract—In conventional backscatter communication (BackCom) systems, time division multiple access (TDMA) and frequency division multiple access (FDMA) are generally adopted for multiuser backscattering due to their simplicity in implementation. However, as the number of backscatter devices (BDs) proliferates, there will be a high overhead under the traditional centralized control techniques, and the inter-user coordination is unaffordable for the passive BDs, which are of scarce concern in existing works and remain unsolved. To this end, in this paper, we propose a slotted ALOHA-based random access for BackCom systems, in which each BD is randomly chosen and is allowed to coexist with one active device for hybrid multiple access. To excavate and evaluate the performance, a resource allocation problem for max-min transmission rate is formulated, where transmit antenna selection, receive beamforming design, reflection coefficient adjustment, power control, and access probability determination are jointly considered. To deal with this intractable problem, we first transform the objective function with the max-min form into an equivalent linear one, and then decompose the resulting problem into three sub-problems. Next, a block coordinate descent (BCD)-based greedy algorithm with a penalty function, successive convex approximation, and linear programming are designed to obtain sub-optimal solutions for tractable analysis. Simulation results demonstrate that the proposed algorithm outperforms benchmark algorithms in terms of transmission rate and fairness.

Index Terms—Hybrid active and passive multiple access, backscatter communication, slotted ALOHA.

I. INTRODUCTION

As massive wireless devices are continuously connected to the Internet, the development of human society has been moved from the period of information revolution represented by the Internet to the period of intelligent revolution represented by the Internet of Things (IoT), heralding the opening of the door to the Internet of Everything [1], [2]. By 2024, a forecast shows that the number of IoT devices will reach 83 billion, which will be a strong contributor to making everything connected [3]. However, the other side of the coin

is that worries have multiplied about how to supply power to such huge amounts of devices for IoT in light of the current energy crunch and the non-negligible energy consumption of each device [4]. As a result, it is an urgent matter to reduce the energy consumption of IoT devices.

Backscatter communication (BackCom), as a cost-, spectrum-, and energy-efficient communication technology, promises to solve the energy supply problem [5]. Specially, wireless devices can adjust the reflection coefficient (RC) by changing the impedance, thus reflecting and modulating the incident radio-frequency (RF) signal from a dedicated signal source without the carrier signal generated by oscillators. Thus, it avoids demodulation and decoding, and requires no additional RF components, which prompts the circuit power consumption of BackCom several orders of magnitude less than that of conventional communications. Along with the evolution of BackCom, ambient backscatter communication (AmBack) inherits the hallmarks of BackCom, and differs from the former in that AmBack is allowed to utilize the surrounding RF sources or systems like cellular base stations (BSs), digital television transmitters, Wi-Fi access points, frequency modulation (FM) signals, LoRa signals, and Bluetooth signals [6].

A. Related Works

1) **Interference-free multiple access:** In the AmBack/BackCom system, it cannot be overlooked that, the backscattered signal undergoes double-channel fading, which is to blame for the vulnerable signal at the receiver. That is to say, both the signals from other backscatter devices (BDs) (namely, backscattering links) and from the RF source (namely, direct link (DL)) are destructive to the current backscattering signal. Therefore, it is hard to overstate the importance to reduce the impacts of interference and improve the performance of the transmission for the AmBack/BackCom. In particular, to circumvent the destruction on backscattering transmission imposed by the DL interference (DLI), interference subtraction [7] and opportunistic successive interference cancellation (SIC) [8] have been applied to the AmBack/BackCom as pivotal techniques to deal with the interference issue. On the other hand, to create an interference-free environment in multi-BD scenarios, time division multiple access (TDMA) has been widely applied in the AmBack/BackCom to avoid the interference generated by concurrent transmission

Bowen Gu, Hao Xie, and Dong Li are with the Faculty of Information Technology, Macau University of Science and Technology, Avenida Wai Long, Taipa, Macau 999078, China (e-mails: 21098538ii30001@student.must.edu.mo, 3220005631@student.must.edu.mo, dli@must.edu.mo).

Ye Liu is with the College of Artificial Intelligence, Nanjing Agricultural University, Nanjing 210031, China, and also with the School of Computer Science and Engineering, Macau University of Science and Technology, Avenida Wai Long, Taipa, Macau 999078, China. (e-mail: yeliu@njau.edu.cn).

Yongjun Xu is with the School of Communication and Information Engineering, Chongqing University of Posts and Telecommunications, Chongqing 400065, China (e-mails: xuyj@cqupt.edu.cn).

among BDs, in which each BD was allowed to backscatter information by turns [9]–[12]. Besides, the frequency shift has been also widely adopted to mitigate the mutual interference among BDs so that backscattering signals can be shifted to the non-overlapping frequency bands for interference avoidance [13]–[15].

2) Spectrum sharing via the hybrid active and passive mode: Conventional AmBack/BackCom systems rely on dedicated or surrounding energy sources to carry tag signals for backscattering. However, it is not always available to obtain such dedicated energy sources and the surrounding energy signals may not be always stable. One possible solution to circumvent these problems is to allow passive BDs to coexist with traditional active users/systems to share the same spectrum. There have been already some works regarding hybrid active and passive users in the spectrum sharing scenarios. In [16]–[18], the BD was incorporated into traditional active transmitter devices so that the adaptive switch between the active and passive mode selection is made possible. By integrating both active and passive devices for spectrum sharing, the system performance can be guaranteed but without any additional transmit power or channel bandwidth resources. In [19]–[21], the spectrum sharing between active and passive devices was considered, where the active devices (ADs) served as energy sources for BDs, and BDs were responsible for protecting the ADs from harmful interference similar to the principle of cognitive radio.

B. Motivations and Contributions

Although traditional multi-access schemes, i.e., TDMA and FDMA, are generally adopted in AmBack/BackCom systems, it may be unaffordable for the passive devices to coordinate each other proactively [22]. A centralized central controller can assist in deconflicting this situation, in which there is however an essential prerequisite that the BS perfectly knows all channel information without the overhead or a small number of devices is involved for optimization [23]. However, in view of the proliferating number of wireless devices, maintaining centralized control is quite challenging, so it is necessary to explore an access protocol with a low overhead and a low complexity.

To this end, random access has recently been revisited and regarded as a vital technology for the medium access control (MAC) layer of the massive IoT. To be more specific, there are unique benefits that can be demonstrated by the random access, such as low latency for small payload transmission, without requiring initial connection setup, dedicated resource allocation for connection maintenance, or signaling overhead for radio resource allocation [24]. Among them, the slotted ALOHA is indisputably one of the finest protocols for random access, which avoids collisions due to partially overlapping transmissions, while retaining a low complexity.

Motivated by the above observations, in this paper, we concentrate on investigating the slotted ALOHA-based random access for the hybrid active and passive multiple access, in which one AD and multiple BDs are able to share the same radio spectrum to simultaneously transmit information to the receiver, and only one BD is allowed to backscatter its

TABLE I
ABBREVIATIONS

Notation	Meaning
AD	Active device
AmBack	Ambient backscatter
AWGN	Additive Gaussian white noise
BackCom	Backscatter communication
BCD	Block coordinate descent
BD	Backscatter devise
BS	Base station
CAP	Channel access probability
CU	Cellular users
CSCG	Circularly symmetric complex Gaussian
DC	Difference-of-convex
DL	Direct link
DLI	Direct-link interference
EH	Energy harvesting
FDMA	Frequency division multiple access
IoT	Internet of Things
LP	Linear programming
MAC	Medium access control
PSD	Positive semi-definite
QoS	Quality-of-service
RC	Reflection coefficient
RF	Radio frequency
SCA	Successive convex approximation
SIC	Successive interference cancellation
SINR	Signal-to-interference-plus-noise ratio
SDR	Semi-definite Relaxation
SNR	Signal-to-noise ratio
TA	Transmit antenna
TAS	Transmit antenna selection
TDMA	Time division multiple access

information at a time. It is worth mentioning that the slotted ALOHA is employed for the first time to control the access of each BD in this paper, which is in contrast to the existing works using TDMA (see, e.g., [9]–[12]) and FDMA (see, e.g., [13]–[15]). Although the concept of random access is also involved in [22], in which each BD could precode its data by multiplying with a random spreading code and backscatter the incident signal, so that the need of the coordination among BDs could be also avoided. However, this work ignores the issue of weak signal decoding performance caused by the concurrent transmission among multiple BDs. In order to avoid this problem, we focus on the single BD case for interference-free random access.

In a nutshell, the main contributions of this paper are summarized as follows:

- A slotted ALOHA-based random access protocol is integrated for the hybrid active and passive multiple access, where multiple BDs share the same spectrum with an AD and each BD is accessed by obeying an independent probability. The considered system can not only circumvent the problem incurred by the coordination-free passive devices, but also effectively avoid mutual interference

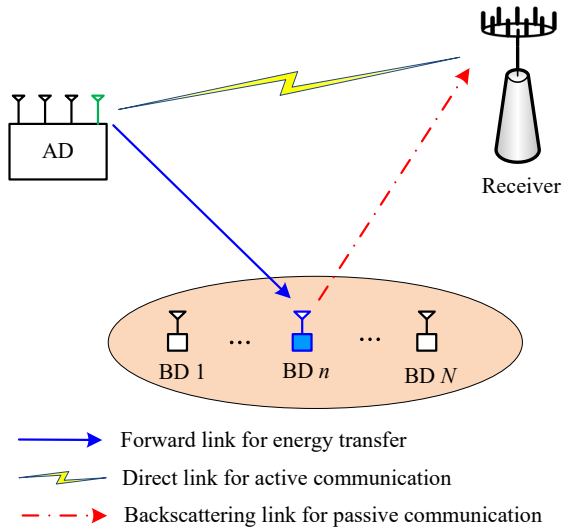


Fig. 1. A hybrid active-passive AmBack system with multiple BDs.

among BDs.

- Our purpose is to maximize the minimum transmission rate for the hybrid active and passive multiple access with the proposed protocol via joint transmit antenna selection (TAS), beamforming design, RC adjustment, power control, and access probability determination. However, the resulting problem is non-convex and challenging to solve. In order to circumvent this difficulty, we first transform the objective function with the max-min form into an equivalent linear one by using a slack variable, and decompose the resulting problem into three sub-problems. Then, a block coordinate descent (BCD)-based greedy algorithm with the penalty method, successive convex approximation (SCA), and linear programming (LP) is proposed to obtain sub-optimal solutions.
- Simulation results demonstrate that the proposed algorithm outperforms benchmark algorithms in terms of transmission performance and fairness.

C. Organization

The remainder of the paper is organized as follows: In Section II, we present the system model and formulate an optimization problem. In Section III, a BCD-based algorithm is proposed to solve the formulated problem. Section IV gives the simulation results, and Section V concludes this paper.

D. Notations

Throughout the paper, scalars, vectors, and matrices are denoted by lowercase, boldface lowercase, and boldface uppercase letters, respectively. $|\cdot|$ and $\|\cdot\|$ denote the absolute value of a complex scalar and the l_2 -norm of a vector, respectively. $(\cdot)^H$, $\text{Rank}(\cdot)$, $\text{Tr}(\cdot)$, $\|\cdot\|_*$, and $\|\cdot\|_2$ represent the Hermitian, the rank, and the trace, the nuclear norm, and the spectral norm of the matrix, respectively. $\delta_i(\cdot)$ denotes the i -th largest singular value of the matrix. \mathbf{I}_K represents the $K \times K$ identity matrix. $\mathbb{E}[\cdot]$ is the statistical expectation. $\mathcal{CN}(\mu, \sigma^2)$ is the circularly symmetric complex Gaussian (CSCG) distribution

with mean μ and variance σ^2 . $[\cdot]^+ = \max(0, \cdot)$ denotes the non-negative value. The abbreviations in this paper are summarized in Table I.

II. SYSTEM MODEL AND PROBLEM FORMULATION

A. System Model

We consider a slotted ALOHA-based BackCom-assisted system, as shown in Fig. 1, which consists of one AD with M transmit antennas (TAs) (i.e., $m \in \mathcal{M} = \{1, 2, \dots, M\}$), N single-antenna BDs (i.e., $n \in \mathcal{N} = \{1, 2, \dots, N\}$), and one receiver with K receive antennas. Specifically, the AD needs to communicate actively with the receiver, while N BDs backscatter information in a passive manner, which is contingent on the AD. It is assumed that only one TA of the AD can be selected to transmit information at one slot to reduce energy consumption. Considering BDs belong to passive devices, which cannot be colluded in advance, the slotted ALOHA is applied to control the access of BDs. Assuming that channels between the transmitter and the receiver follow a block-fading model, namely, the corresponding channel gains remain constant in one time interval, but vary independently in different intervals. Each BD is assumed to always have information to send, in the corresponding transmission duration, the decision of the n -th BD on whether to access the channel is determined by the outcome of a Bernoulli experiment, modeled by a random variable $I_n \in \{0, 1\}$, which is realized locally at the n -th BD [25]. When $I_n = 1$ holds, the n -th BD transmits information, and it is silent otherwise, i.e.,

$$I_n = \begin{cases} 1, & \text{with probability } q_n, \\ 0, & \text{with probability } 1 - q_n, \end{cases} \quad (1)$$

where $\mathbb{E}[I_n] = q_n$, $\mathbb{E}[1 - I_n] = 1 - q_n$, and q_n is the channel access probability (CAP) of the n -th BD. It is assumed that only one BD can be accessed at one time to avoid the mutual interference. That is to say, a transmission collision will occur when two or more BDs transmit information at the same time, and it is regarded as successful transmission only and only if there is only one BD backscattering its information, in which the successful probability for backscattering of the n -th BD is equal to $q_n \prod_{j \neq n} (1 - q_j)$.

B. Energy Harvesting

When the m -th TA of the AD is used, the received signal at the n -th BD can be expressed as

$$y_{m,n}^{\text{BD}} = \sqrt{P_m} h_{m,n}^f s_m + w_n, \forall m, n, \quad (2)$$

where s_m is transmitted symbol by the m -th TA of the AD, satisfied $\mathbb{E}(|s_m|^2) = 1$. P_m denotes the transmit power of the m -th TA of the AD. $h_{m,n}^f$ denotes the channel coefficient from the m -th TA of the AD to the n -th BD. $w_n \sim \mathcal{CN}(0, \sigma_n^2)$ is the additive Gaussian white noise (AWGN), and σ_n^2 denotes the noise power at the n -th BD.

It is worth stating that since each BD is passive, its received signal needs to be divided into two parts, one to serve the communication demands and the other to serve as an energy signal for its circuit operation. Thus, based on (2),

the harvested power for the operation support of the n -th BD from the m -th TA can be expressed as

$$P_n^{\text{EH}} = (1 - \alpha_n) \sum_{m=1}^M \beta_m P_m |h_{m,n}^f|^2, \forall n, \quad (3)$$

where α_n is the RC of the n -th BD. β_m denotes the TA selection (TAS) factor, i.e., when the m -th TA is selected, $\beta_m = 1$; otherwise, $\beta_m = 0$.

To be more practical, a non-linear energy harvesting (EH) model is considered (see, i.e., [11]), and thus the harvested energy of the n -th BD can be expressed as

$$\begin{aligned} & \Phi_n(P_n^{\text{EH}}) \\ &= \left[\frac{P_n^{\text{SA}}}{\exp(-a_n P_n^{\text{SE}} + b_n)} \left\{ \frac{1 + \exp(-a_n P_n^{\text{SE}} + b_n)}{1 + \exp(-a_n P_n^{\text{EH}} + b_n)} - 1 \right\} \right]^+, \forall m, n \end{aligned} \quad (4)$$

where $\Phi_n(P_n^{\text{EH}})$ is the actual power that can be harvested by the n -th BD. P_n^{SA} and P_n^{SE} denote the thresholds of EH saturation and the EH sensitivity for the n -th BD, respectively. Moreover, a_n and b_n are constants that can control the steepness of $\Phi_n(P_n^{\text{EH}})$ [26].

C. Information Transmission

When the m -th TA of the AD is selected and the n -th BD is accessed, the received signals at the receiver can be expressed as

$$\mathbf{x}_{m\&n}^{\text{R}} = \underbrace{\sqrt{P_m} \mathbf{h}_m^{\text{d}} s_m}_{\text{direct link}} + \underbrace{\sqrt{\alpha_n} \sqrt{P_m} h_{m,n}^f \mathbf{h}_n^{\text{b}} s_m c_n}_{\text{backscattering link}} + \mathbf{w}^{\text{R}}, \forall m, n, \quad (5)$$

where c_n is the transmitted symbol by the n -th BD, satisfying $\mathbb{E}[|c_n|^2] = 1$. $\mathbf{h}_m^{\text{d}} \in \mathbb{C}^{K \times 1}$ and $\mathbf{h}_n^{\text{b}} \in \mathbb{C}^{K \times 1}$ denote the channel vectors of the m -th TA-receiver link and the BD n -receiver link, respectively. $\mathbf{w}^{\text{R}} \in \mathbb{C}^{K \times 1}$ denotes the noise vector of the receiver and is assumed to be a circularly symmetric complex Gaussian (CSCG) random vector with $\mathbf{w}^{\text{R}} \sim \mathcal{CN}(0, \sigma_w^2 \mathbf{I}_K)$. σ_w^2 denotes the noise power. By adopting the receiver beamforming, we have

$$\begin{aligned} y_{m\&n}^{\text{R}} &= \mathbf{v}_{m\&n}^{\text{H}} \mathbf{x}_{m\&n}^{\text{R}} \\ &= \mathbf{v}_{m\&n}^{\text{H}} \sqrt{P_m} \mathbf{h}_m^{\text{d}} s_m + \sqrt{\alpha_n} \sqrt{P_m} h_{m,n}^f \mathbf{v}_{m\&n}^{\text{H}} \mathbf{h}_n^{\text{b}} s_m c_n \\ &\quad + \mathbf{v}_{m\&n}^{\text{H}} \mathbf{w}^{\text{R}}, \forall m, n, \end{aligned} \quad (6)$$

where $\mathbf{v}_{m\&n} \in \mathbb{C}^{K \times 1}$ denotes the beamforming vector at the receiver, satisfying $\|\mathbf{v}_{m\&n}\|^2 = 1$.

It is noted that the backscattering signal undergoes double-path loss, which is to blame for the signal strength of the backscattering link to be much weaker than that of the DL. As a result, the receiver can first decode the DL signal from y_m via SIC, then cancels out the decoded signal from y_m , and finally detects the backscattering signal c_n . That is to say, when decoding the DL signal, the backscattering signal is regarded as the interference. Thus, the signal-to-interference-plus-noise ratio (SINR) of the m -th TA of the AD with the

n -th BD is given by

$$\gamma_{m\&n}^{\text{AD}} = \frac{|\mathbf{v}_{m\&n}^{\text{H}} \mathbf{h}_m^{\text{d}}|^2 P_m}{\alpha_n |h_{m,n}^f|^2 |\mathbf{v}_{m\&n}^{\text{H}} \mathbf{h}_n^{\text{b}}|^2 P_m + \sigma_w^2}, \forall m, n. \quad (7)$$

The achievable throughput of the AD with the n -th accessed BD is given by

$$R_n^{\text{AD}} = q_n \prod_{j \neq n} (1 - q_j) \sum_{m=1}^M \beta_m r_{m\&n}^{\text{AD}}, \forall m, n, \quad (8)$$

where $r_{m\&n}^{\text{AD}} = \log_2(1 + \gamma_{m\&n}^{\text{AD}})$.

On the other hand, when decoding the backscattering signal, the DL signal can be regarded as perfectly removing from $y_{m\&n}$ via SIC. Thus, the received signal from the n -th BD at the receiver can be expressed as

$$\bar{y}_{m\&n}^{\text{R}} = \sqrt{\alpha_n} \sqrt{P_m} h_{m,n}^f \mathbf{v}_{m\&n}^{\text{H}} \mathbf{h}_n^{\text{b}} s_m c_n + \mathbf{v}_{m\&n}^{\text{H}} \mathbf{w}^{\text{R}}, \forall m, n. \quad (9)$$

According to (9), the signal-to-noise ratio (SNR) for the n -th BD can be expressed as

$$\gamma_{m\&n}^{\text{BD}} = \frac{\alpha_n |h_{m,n}^f|^2 |\mathbf{v}_{m\&n}^{\text{H}} \mathbf{h}_n^{\text{b}}|^2 P_m}{\sigma_w^2}, \forall m, n. \quad (10)$$

The achievable throughput of the n -th BD is given by

$$R_n^{\text{BD}} = q_n \prod_{j \neq n} (1 - q_j) \sum_{m=1}^M \beta_m r_{m\&n}^{\text{BD}}, \forall m, n, \quad (11)$$

where $r_{m\&n}^{\text{BD}} = \log_2(1 + \gamma_{m\&n}^{\text{BD}})$.

D. Problem Formulation

The purpose is to find a fair transmission scheme with slotted ALOHA for hybrid multiple access by optimizing the TAS factor and transmit power of the AD, the CAP and RC of each BD, as well as the receiver beamforming vector, where the quality-of-service (QoS) requirements of the AD, and the EH demands of BDs are taken into account. Thus, the optimization problem can be formulated as

$$\begin{aligned} & \max_{\beta_m, q_n, P_m, \alpha_n, \mathbf{v}_{m\&n}} \min_{\forall n} R_n^{\text{BD}} \\ \text{s.t. } & C_1 : \beta_m \in \{0, 1\}, \sum_m \beta_m = 1, \\ & C_2 : 0 < q_n < 1, \forall n, \\ & C_3 : R_n^{\text{AD}} \geq R_n^{\text{min}}, \forall n, \\ & C_4 : \Phi_n(P_n^{\text{EH}}) \geq P_n^{\text{C}}, \forall n, \\ & C_5 : 0 < \alpha_n \leq 1, \forall n, \\ & C_6 : \sum_{m=1}^M \beta_m P_m \leq P^{\text{max}}, \\ & C_7 : \|\mathbf{v}_{m\&n}\|^2 = 1, \forall m, n, \end{aligned} \quad (12)$$

where R_n^{min} denotes the minimum required throughput of the AD with the n -th accessed BD. P_n^{C} is the circuit power of the n -th BD. P^{max} represents the maximum transmit power of the AD. It is worth detailing that C_1 can guide the selection factors for TAs, which means that only one TA can be selected for transmission. C_2 is used to limit the CAP of each BD. C_3

can ensure the QoS requirement of the AD. C_4 guarantees that the harvested energy of the n -th BD is sufficient to maintain its operation. C_5 and C_6 impose limitations on the RC of the n -th BD and the transmit power of the m -th TA of the AD, respectively. C_7 qualifies the receive beamforming vectors.

III. ALGORITHM DESIGN

It can be seen that it is intractable to solve problem (12), due to the non-convexity caused by the non-smooth objective function and the coupling of variables. To deal with it, we first remove the max-min form from the objective function using a slack variable. Second, the resulting problem is decomposed into three sub-problems, and different algorithms are designed to solve them separately. Finally, according to the BCD-based greedy method, problem (12) is solved by alternating optimizing these three sub-problems.

A. Problem Reformulation

It is hard to solve problem (12) due to the non-smooth objective function posed by the max-min form. To deal with this, a slack variable t is introduced, such that $\min_{\forall n} R_n^{\text{BD}} \geq t$. As a result, problem (12) can be transformed into

$$\begin{aligned} & \max_{\beta_m, q_n, P_m, \alpha_n, \mathbf{v}_{m\&n}, t} t \\ & \text{s.t. } C_1 \sim C_7, \\ & C_8 : R_n^{\text{BD}} \geq t, \forall n. \end{aligned} \quad (13)$$

It is observed that problem (13) involves both binary and continuous variables, and there exist strong coupled relationships of optimization variables among constraints. In general, for such a non-convex problem, it is very difficult to solve its optimal solution directly. This motivates us to design a BCD-based greedy algorithm to solve it. Specifically, problem (13) is decomposed into three sub-problems, namely, the sub-problem for beamforming design, the sub-problem for power control and RC optimization, and the sub-problem for CAP determination.

B. The Sub-problem for Beamforming Design

With fixed β_m , P_m , q_n , and α_n , the sub-problem for beamforming design can be formulated as

$$\begin{aligned} & \max_{\mathbf{v}_{m\&n}, t} t \\ & \text{s.t. } C_3, C_7, C_8. \end{aligned} \quad (14)$$

However, problem (14) is still non-convex due to the non-convexity of the transmission rates of the AD and the n -th BD. To make it tractable, a new variable is applied, such as $\mathbf{V}_{m\&n} = \mathbf{v}_{m\&n} \mathbf{v}_{m\&n}^H$, problem (14) can be equivalently rewritten by

$$\begin{aligned} & \max_{\mathbf{V}_{m\&n}, t} t \\ & \text{s.t. } \bar{C}_3 : \left(2^{\bar{R}_n^{\text{min}}} - 1\right) \left(\text{Tr}(\mathbf{H}_n^{\text{b}} \mathbf{V}_{m\&n}) \alpha_n |h_{m,n}^{\text{f}}|^2 P_m + \sigma_w^2\right) \\ & \leq \text{Tr}(\mathbf{H}_m^{\text{d}} \mathbf{V}_{m\&n}) P_m, \forall n, \\ & \bar{C}_7 : \text{Tr}(\mathbf{V}_{m\&n}) = 1, \forall n, \end{aligned} \quad (15)$$

$$\begin{aligned} \bar{C}_8 : & \log_2 \left(1 + \frac{\text{Tr}(\mathbf{H}_n^{\text{b}} \mathbf{V}_{m\&n}) \alpha_n |h_{m,n}^{\text{f}}|^2 P_m}{\sigma_w^2}\right) \\ & \cdot q_n \prod_{j \neq n} (1 - q_j) \geq t, \forall n, \\ \bar{C}_9 : & \text{Rank}(\mathbf{V}_{m\&n}) = 1, \forall n, \end{aligned}$$

where $\bar{R}_n^{\text{min}} \triangleq \frac{R_n^{\text{min}}}{q_n \prod_{j \neq n} (1 - q_j)}$, $\mathbf{H}_m^{\text{d}} = \mathbf{h}_m^{\text{d}} (\mathbf{h}_m^{\text{d}})^H$, and $\mathbf{H}_n^{\text{b}} = \mathbf{h}_n^{\text{b}} (\mathbf{h}_n^{\text{b}})^H$.

It is noted that the rank-one constraint C_9 is an impediment to solving problem (15). Semi-definite relaxation (SDR) has been commonly adopted to tackle the rank-one constraint, which, however, may not result in a rank-one matrix. Moreover, some approximation methods, such as Gaussian randomization, may cause performance deterioration when the number of antennas is quite large [27]. To deal with this, C_9 is equivalently transformed into the following difference-of-convex (DC) function [28], such as

$$\bar{C}_9 : \|\mathbf{V}_{m\&n}\|_* - \|\mathbf{V}_{m\&n}\|_2 = 0, \forall n, \quad (16)$$

where $\|\mathbf{X}\|_* = \sum_i \delta_i(\mathbf{X})$ and $\|\mathbf{X}\|_2 = \delta_1(\mathbf{X})$. A simple proof is as follows: It is noted that for any \mathbf{X} belonging to the positive semi-definite (PSD) matrix, $\|\mathbf{X}\|_* \geq \|\mathbf{X}\|_2 = \max_i \delta_i(\mathbf{X})$ is always held. The inequality can be treated as an equation if and only if \mathbf{X} is a rank-one matrix, especially, $\delta_1(\mathbf{X}) = \|\mathbf{X}\|_2$ and $\delta_i(\mathbf{X}) = 0, \forall i = 2, \dots, N$. As a result, (16) can be efficiently met for the rank-one constraint C_9 . However, (16) is still non-convex. To deal with it, a penalty function is employed, and thus problem (15) can be equivalently transformed into the following problem [29], i.e.,

$$\begin{aligned} & \max_{\mathbf{V}_{m\&n}, t} t - \chi (\|\mathbf{V}_{m\&n}\|_* - \|\mathbf{V}_{m\&n}\|_2) \\ & \text{s.t. } \bar{C}_3, \bar{C}_7, \bar{C}_8, \end{aligned} \quad (17)$$

where \bar{C}_9 is relaxed to a penalty term added to the objective function, and χ is a constant which penalizes the objective function for any matrix whose rank is not one.

However, problem (17) is still an intractable problem with any $\chi > 0$ due to the non-convexity of the objective function. To deal with this, the SCA-based method is introduced in this paper. Specifically, for a given $\mathbf{V}_{m\&n}(e)$ in the e -th iteration of SCA, a convex upper bound for the penalty term can be obtained by using first-order Taylor expansion, which can be expressed as

$$\|\mathbf{V}_{m\&n}\|_* - \|\mathbf{V}_{m\&n}\|_2 \leq \|\mathbf{V}_{m\&n}\|_* - \|\bar{\mathbf{V}}_{m\&n}(e)\|, \quad (18)$$

where $\bar{\mathbf{V}}_{m\&n}(e) \triangleq \|\mathbf{V}_{m\&n}(e)\|_2 + \text{Tr}[\bar{\mathbf{u}}(\mathbf{V}_{m\&n}(e)) (\bar{\mathbf{u}}(\mathbf{V}_{m\&n}(e)))^H (\mathbf{V}_{m\&n} - \mathbf{V}_{m\&n}(e))]$ and $\bar{\mathbf{u}}(\mathbf{V}_{m\&n}(e))$ represents the eigenvector corresponding to the largest eigenvalue of $\mathbf{V}_{m\&n}(e)$.

As a result, problem (17) can be finally rewritten as

$$\begin{aligned} & \max_{\mathbf{V}_{m\&n}, t} t - \chi (\|\mathbf{V}_{m\&n}\|_* - \bar{\mathbf{V}}_{m\&n}(e)) \\ & \text{s.t. } \bar{C}_3, \bar{C}_7, \bar{C}_8. \end{aligned} \quad (19)$$

Note that problem (19) is a convex optimization problem and its solution can be obtained via CVX [30]. The proposed

$$P_m^* = P^{\max} > \max \left\{ \frac{\Phi_n^{-1}(P_n^C)}{|h_{m,n}^f|^2}, \frac{(2^{\bar{R}_n^{\min}} - 1) \sigma_w^2}{\text{Tr}(\mathbf{H}_m^d \mathbf{V}_{m\&n})} \right\} \triangleq P_{m\&n}^{\min}, \forall n, \quad (21a)$$

$$\alpha_n^* = \left[\min \left\{ \underbrace{\frac{\text{Tr}(\mathbf{H}_m^d \mathbf{V}_{m\&n}) P^{\max} - (2^{\bar{R}_n^{\min}} - 1) \sigma_w^2}{(2^{\bar{R}_n^{\min}} - 1) \text{Tr}(\mathbf{H}_n^b \mathbf{V}_{m\&n}) |h_{m,n}^f|^2 P^{\max}}}_{\alpha_n^{\text{AD}}}, \underbrace{1 - \frac{\Phi_n^{-1}(P_n^C)}{P^{\max} |h_{m,n}^f|^2}}_{\alpha_n^{\text{EH}}} \right\} \right]^+, \forall n. \quad (21b)$$

$$t_n^* = \begin{cases} q_n \prod_{j \neq n} (1 - q_j) \log_2 \left(1 + \frac{\text{Tr}(\mathbf{H}_m^d \mathbf{V}_{m\&n}) P^{\max} - (2^{\bar{R}_n^{\min}} - 1) \sigma_w^2}{(2^{\bar{R}_n^{\min}} - 1) \sigma_w^2} \right), & \alpha_n^{\text{AD}} \leq \alpha_n^{\text{EH}}, \forall n, \\ q_n \prod_{j \neq n} (1 - q_j) \log_2 \left(1 + \frac{\text{Tr}(\mathbf{H}_n^b \mathbf{V}_{m\&n}) (P^{\max} |h_{m,n}^f|^2 - \Phi_n^{-1}(P_n^C))}{\sigma_w^2} \right), & \alpha_n^{\text{AD}} \geq \alpha_n^{\text{EH}}, \forall n. \end{cases} \quad (22)$$

Algorithm 1 The Algorithm for Solving Problem (19)

Fixed: $\alpha_n, \beta_m, P_m, q_n$.

Set: Set the iteration index $e = 1$, the tolerance ω , the maximum iteration number E , and the initial point $\mathbf{V}_{m\&n}(0)$.

- 1: **while** $|\mathbf{V}_{m\&n}(e+1) - \mathbf{V}_{m\&n}(e)| \geq \omega$ or $e \leq E$ **do**
 - 2: Given $\mathbf{V}_{m\&n}(e)$, solve problem (19) by using CVX to obtain $\mathbf{V}_{m\&n}(e+1)$ and $t(e)$.
 - 3: $e = e + 1$.
 - 4: **end while**
 - 5: Obtain the solution to problem (16) as $\mathbf{V}_{m\&n}^* = \mathbf{V}_{m\&n}(e)$ and $t^* = t(e)$.
-

algorithm for solving (19) is summarized in **Algorithm 1**.

C. The Sub-problem for Power Control and RC Optimization

With fixed q_n, β_m , and $\mathbf{V}_{m\&n}$, the sub-problem for power control and RC optimization can be formulated as

$$\begin{aligned} & \max_{P_m, \alpha_n, t'} \\ & \text{s.t. } \bar{C}_3, C_5, C_6, \\ & \bar{C}_4 : (1 - \alpha_n) P_m |h_{m,n}^f|^2 \geq \Phi_n^{-1}(P_n^C), \forall n, \\ & \tilde{C}_8 : \log_2 \left(1 + \frac{\text{Tr}(\mathbf{H}_n^b \mathbf{V}_{m\&n}) \alpha_n |h_{m,n}^f|^2 P_m}{\sigma_w^2} \right) \\ & \quad \cdot q_n \prod_{j \neq n} (1 - q_j) \geq t', \forall n, \end{aligned} \quad (20)$$

where $\Phi_n^{-1}(x) = \left[\frac{b_n - \ln A_n}{a_n} \right]^+$ is the inverse function of Φ_n , $A_n = \frac{1 + \exp(-a_n P_n^{\text{SE}} + b_n)}{B_n x + 1} - 1$, and $B_n = \frac{\exp(-a_n P_n^{\text{SE}} + b_n)}{P_n^{\text{SA}}}$.

It can be seen that problem (20) is non-convex due to the tightly coupled variables in the objective function and constraints. To solve this problem, we propose the following lemma.

Lemma: With fixed q_n, β_m , and $\mathbf{V}_{m\&n}$, the optimal P_m^* and α_n^* can be derived as (21a) and (21b), respectively.

Proof: Please see Appendix A.

Remark: The lower bound for P^{\max} is given by (21a), which can guide us in setting the maximum transmit power of the AD, whose value should be at least higher than this lower bound. From (21b), it can be seen that α_n^{AD} decreases with the increasing $|h_{m,n}^f|^2$ and/or the decreasing $\text{Tr}(\mathbf{H}_m^d \mathbf{V}_{m\&n})$. The reason is that the enhanced backscattering link and/or the decreased direct link brings more interference for the AD, thus the RC of the accessed BD has to decrease to satisfy the QoS of the AD. Besides, α_n^{AD} also decreases with the increasing \bar{R}_n^{\min} since when \bar{R}_n^{\min} increases, the corresponding SINR for the AD also increases, which reduces the tolerance for interference signal. On the other hand, α_n^{EH} decreases as P^{\max} and/or $|h_{m,n}^f|^2$ become smaller. This is because the decreasing P^{\max} and/or $|h_{m,n}^f|^2$ make the harvested energy of each BD decrease, and the ratio of energy allocated to compensate for the circuit increases accordingly. In summary, the scale will be biased towards α_n^{AD} when the channel gain of the backscattering link is stronger, or when a higher rate for the AD is desired. Conversely, there is a preference for α_n^{EH} .

Then, the optimal t' for problem (20) can be obtained by substituting (21a) and (21b) into problem (20), which can be expressed as $t^* = \min t_n^*$, where t_n^* is expressed as (22).

D. The Sub-problem for CAP Determination

Let us consider q_n in this subsection with the fixed β_m, α_n, P_m , and $\mathbf{V}_{m\&n}$. The sub-problem for CAP determination can be expressed as

$$\begin{aligned} & \max_{q_n, t''} \\ & \text{s.t. } C_1, C_2, \bar{C}_4, \\ & \tilde{C}_3 : q_n \prod_{j \neq n} (1 - q_j) \bar{r}_{m\&n}^{\text{AD}} \geq R_n^{\min}, \forall n, \\ & \hat{C}_8 : q_n \prod_{j \neq n} (1 - q_j) \bar{r}_{m\&n}^{\text{BD}} \geq t'', \forall n, \end{aligned} \quad (23)$$

Algorithm 2 The Algorithm for Solving Problem (27)

Fixed: $\beta_m, \alpha_n, P_m, \mathbf{V}_{m\&n}$.

Set: Set the iteration index $d = 1$, the tolerance ϕ , the maximum iteration number D , and the initial point $x_n(0), y_n(0)$, and $z(0) = 0$.

- 1: **while** $|z(d+1) - z(d)| \geq \phi$ or $d \leq D$ **do**
 - 2: Given $x_n(d)$ and $y_n(d)$, solve problem (27) via LP to obtain $x_n(d), y_n(d)$, and $z(d)$.
 - 3: $d = d + 1$.
 - 4: **end while**
 - 5: Obtain the solution to problem (27) as $q_n^* = \exp(x_n(d))$ and $(t'')^* = \exp(z(d))$.
-

$$\text{where } \bar{r}_{m\&n}^{\text{AD}} = \log_2 \left(1 + \frac{\text{Tr}(\mathbf{H}_m^{\text{d}} \mathbf{V}_{m\&n}) P_m}{\text{Tr}(\mathbf{H}_n^{\text{b}} \mathbf{V}_{m\&n}) \alpha_n |h_{m,n}^{\text{f}}|^2 P_m + \sigma_w^2} \right) \text{ and}$$
$$\bar{r}_{m\&n}^{\text{BD}} = \log_2 \left(1 + \frac{\text{Tr}(\mathbf{H}_n^{\text{b}} \mathbf{V}_{m\&n}) \alpha_n |h_{m,n}^{\text{f}}|^2 P_m}{\sigma_w^2} \right).$$

However, multivariate decision is an obstacle to solving problem. To make problem (23) treatable, it can be equivalently transformed into

$$\begin{aligned} & \max_{q_n, t''} t'' \\ & \text{s.t. } C_2, \check{C}_3 : \ln q_n + \sum_{j=1, j \neq n}^N \ln(1 - q_j) + \ln \bar{r}_{m\&n}^{\text{AD}} \\ & \quad \geq \ln R_n^{\text{min}}, \forall n, \\ & \check{C}_8 : \ln q_n + \sum_{j=1, j \neq n}^N \ln(1 - q_j) + \ln \bar{r}_{m\&n}^{\text{BD}} \geq \ln t'', \forall n. \end{aligned} \quad (24)$$

However, problem (24) is still challenging due to the non-linearity of the constraints. To deal with it, we make the following transformation, i.e.,

$$\begin{aligned} & \max_{x_n, y_n, z} z \\ & \text{s.t. } \bar{C}_2 : x_n < 0, y_n < 0, \forall n, \\ & \hat{C}_3 : x_n + \sum_{j=1, j \neq n}^N y_j \geq \ln R_n^{\text{min}} - \ln \bar{r}_{m\&n}^{\text{AD}}, \forall n, \\ & \check{C}_8 : x_n + \sum_{j=1, j \neq n}^N y_j \geq z - \ln \bar{r}_{m\&n}^{\text{BD}}, \forall n, \\ & C_{10} : \exp(x_n) + \exp(y_n) = 1, \forall n, \end{aligned} \quad (25)$$

where $x_n = \ln q_n$, $y_n = \ln(1 - q_n)$, and $z = \ln t''$.

Note that problem (25) is still hard to solve due to the non-linearity of C_{10} . In order to linearize the C_{10} , SCA-based method is employed. Specifically, with the first order Taylor approximation, C_{10} can be transformed into

$$\begin{cases} \exp(x_n) = \exp(\bar{x}_n(d))(x_n - \bar{x}_n(d) + 1) \triangleq f(x_n), \\ \exp(y_n) = \exp(\bar{y}_n(d))(y_n - \bar{y}_n(d) + 1) \triangleq g(y_n), \end{cases} \quad (26)$$

where $\bar{x}_n(d)$ and $\bar{y}_n(d)$ are the value of \bar{x}_n and \bar{y}_n at the d -th

Algorithm 3 The Greedy Algorithm for TAS

Input: $K, M, N, h_{m,n}^{\text{f}}, \mathbf{h}_m^{\text{d}}, \mathbf{h}_n^{\text{b}}, \sigma_w^2, \sigma_n^2, R_n^{\text{min}}, P_n^{\text{C}}, P_n^{\text{max}}, P_n^{\text{SA}}, P_n^{\text{SE}}, a_n, b_n$.

Set: Set the tolerance ε , the iteration number $l = 1$, the maximum iteration number L , and the initial point t_0 .

Output: $P_m, \alpha_n, \beta_m, q_n, \mathbf{v}_{m\&n}$.

- 1: **for** $m = 1 : M$
 - 2: Set $\beta_m = 1$.
 - 3: **while** $|t(l) - t'(l)|$ or $|t(l) - t''(l)| > \varepsilon$ or $l \leq L$ **do**
 - 4: Given $\alpha_n(l), P_m(l)$, and $q_n(l)$, solve sub-problem (19) to obtain $\mathbf{v}_{m\&n}(l+1)$ and $t(l+1)$ based on **Algorithm 1**.
 - 5: Given $\mathbf{v}_{m\&n}(l+1)$ and $q_n(l)$, solve sub-problem (20) to obtain $P_m(l+1)$ and $\alpha_n(l+1)$ based on (21a) and (21b), and $t'(l+1)$ based on (22).
 - 6: Given $\alpha_n(l+1), P_m(l+1)$, and $\mathbf{v}_{m\&n}(l+1)$, solve sub-problem (27) to obtain $q_n(l+1)$, and $t''(l+1)$ based on **Algorithm 2**.
 - 7: $l = l + 1$.
 - 8: **end while**
 - 9: Update $t(m) = t(l)$.
 - 10: **if** $t(m) \leq t_0$
 - 11: Set $\beta_m = 0$.
 - 12: **else**
 - 13: Update $t_0 = t(m)$.
 - 14: **end if**
 - 15: **end for**
-

iteration, respectively. Thus, we have

$$\begin{aligned} & \max_{x_n, y_n, z} z \\ & \text{s.t. } \bar{C}_2, \hat{C}_3, \check{C}_8, \\ & \quad \bar{C}_{10} : f(x_n) + g(y_n) = 1, \forall n, \end{aligned} \quad (27)$$

It is worth stating that problem (27) is an LP problem, which can be solved efficiently using the numerical evaluation. The details of this algorithm are given by **Algorithm 2**.

E. The Greedy Algorithm for TAS

In the above subsections, the beamforming vectors, the transmit power of the AD, and the RC and CAP of each BD have been solved separately. How to select the optimal TA for transmission still remains unsolved. In what follows, we will tackle this issue. It is noted that the problem of TAS is a 0-1 non-linear problem, which is NP-complete. This motivates us to design a greedy algorithm to obtain the optimal TAS factor. The overall BCD-based greedy algorithm is summarized in **Algorithm 3**.

IV. SIMULATION RESULTS

In this section, we provide simulation results to evaluate the performance of the proposed algorithm. We assume that there are one AD with 4 transmit antennas, 4 single-antenna BDs,

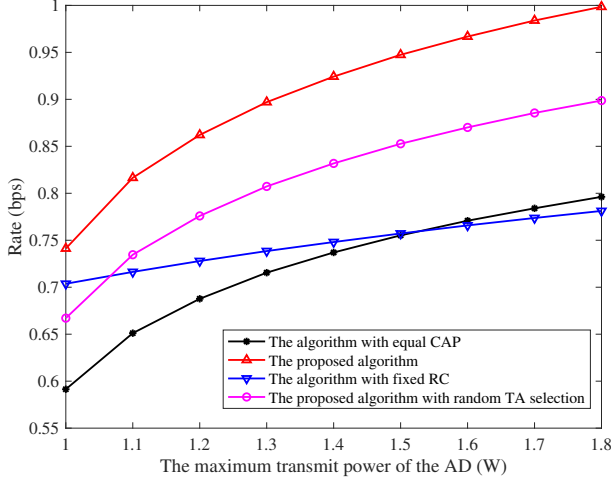


Fig. 2. Rate versus the transmit power of the AD.

and one receiver with 4 antennas in the considered system. The distances between the AD and the receiver is within 6.0 m. Besides, the distances between BDs and the receiver are both within the range of 3.0 m to 5.0 m, and the distances between the AD and BDs are within the range of 3.0 m to 5.5 m. We consider the distance-dependent path loss as large-scale fading, where the path-loss exponent is 2.2, and Rician fading as small-scale fading, where the Rician factor is 2.8 dB. Other parameters include $P^{\max} = 1$ W, $R_n^{\min} = 0.1$ bps, $P_n^C = 1$ mW, $a_n = 274$, $b_n = 0.29$, $P_n^{\text{SE}} = 0.064$ mW, $P_n^{\text{SA}} = 4.927$ mW [26], and $\sigma_n^2 = \sigma_w^2 = 10^{-8}$ W. The iteration termination thresholds ω , ϕ , and ε are both set as 10^{-4} . Besides, the maximum iteration numbers E , D , and L are both set as 10^3 . Finally, the simulation results are based on the CVX package [31]. Next, we evaluate the proposed algorithms in the following two aspects, namely performance and fairness.

A. The Performance of Algorithm

In this subsection, the performance of the proposed algorithms is provided. To better demonstrate this property, three benchmark algorithms are defined and compared, such as

- **The algorithm with equal CAP**

In this algorithm, each BD is endowed with the same CAP, and the CAP of each BD is $\frac{1}{N}$.

- **The algorithm with fixed RC**

In this algorithm, the RC of each BD is set to a constant and no longer changes dynamically.

- **The algorithm with random TA selection**

In this algorithm, the TA is still allowed to access only one, but it is randomly selected.

Fig. 2 illustrates the transmission rate versus the maximum transmit power of the AD. From the figure, it can be obtained that the transmission rate of all algorithms increases with the increase of the transmit power of the AD. This fact can be explained due to the monotonic increasing function of the transmission rate with respect to the transmit power. In addition, the rate of the proposed algorithm is larger than

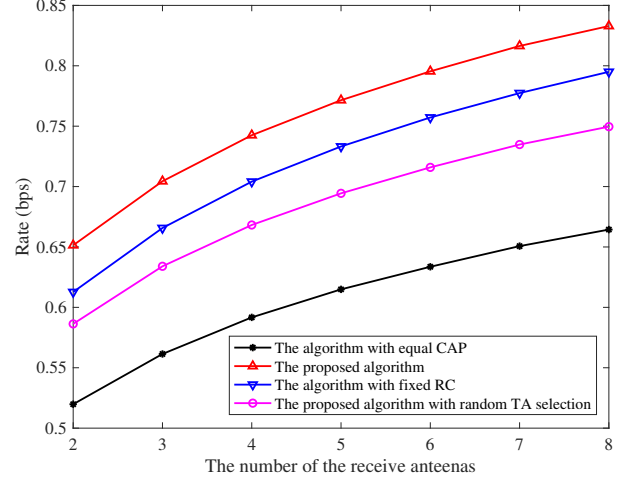


Fig. 3. Rate versus the number of receive antennas.

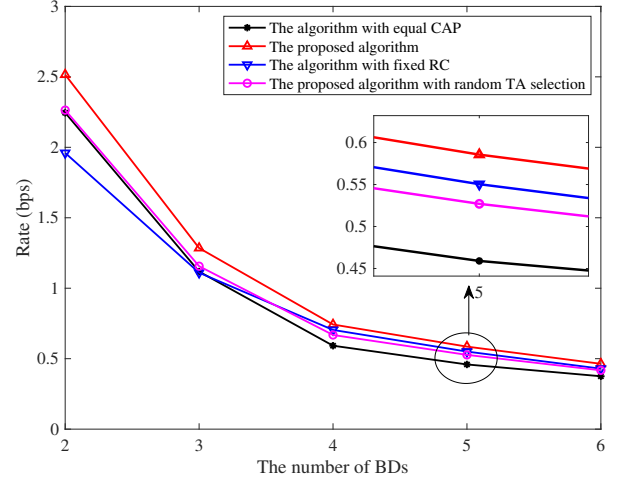


Fig. 4. Rate versus the number of BDs.

that of other algorithms. This is because the algorithms with fixed RC and equal CAP cannot be dynamically adjusted, and thus makes the resource slightly mismatched. Besides, the algorithm with random TA selection has uncertainty and thus does not reliably provide high-quality transmission.

Fig. 3 reveals the transmission rate versus the number of antennas of the receiver. It is observed that the transmission rate of all algorithms increases with the increase of the receive antennas. For this fact it can be explained that the increase of the receive antennas makes the beamforming gain increase and thus the SNR increase. Moreover, the rate of the algorithm with CAP is the lowest. Because this algorithm ignores the channel variability among different BDs, although a fair access probability is guaranteed, the fair resource occupation is sacrificed. Comparing with the algorithm with fixed RC, the proposed algorithm can adjust the RC of each BD, which helps to enhance the backscattering signal power.

Fig. 4 demonstrates the transmission rate versus the number of BDs. As can be seen from the figure, the transmission

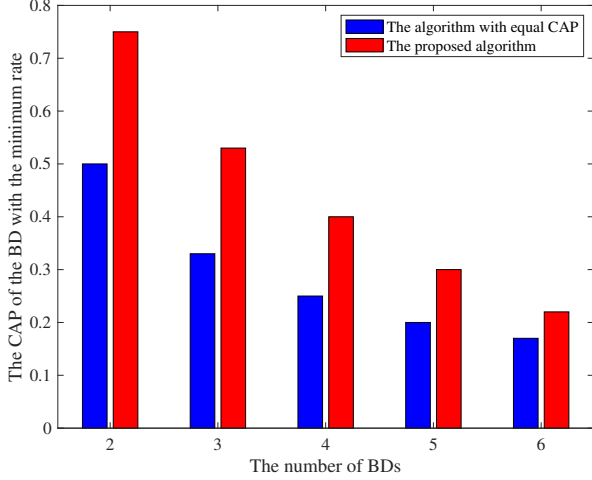


Fig. 5. The CAP versus the number of BDs.

rate for all algorithms gradually decreases, and the rate gap between them diminishes as the number of BDs increases. The reason is that the increasing number of BDs makes the CAP of each BD suppressed, which not only reduces the impact of transmission success probabilities (i.e., $q_n \prod_{j \neq n} (1 - q_j)$) on rate differences between BDs, but also leads to the effective transmission rate becoming low.

Fig. 5 provides the CAP of the BD with minimum rate versus the number of BDs. Not surprisingly, the CAP for two algorithms is gradually decreasing as more BDs are involved. Moreover, the CAP of the proposed algorithm is higher than that of the algorithm with equal CAP. The reason is that the aim of the proposed algorithm is to maximize the minimum rate among BDs, which is inclined to take care of the BDs with the lower rate. Besides, the CAP gap between these two algorithms decreases as the increasing number of BDs. Since the feasible domain of the optimal CAP is also gradually compressed to satisfy the QoS of the active communication. This also complements the phenomenon of the rate becoming closer with the increasing BDs in Fig. 4.

B. The Fairness of Algorithm

In this subsection, the fairness of the proposed algorithms is evaluated. Fig. 6 depicts the transmission rate versus the minimum required rate of the AD. It is seen that as the minimum required rate of the AD increases, the maximum backscattering rate of the algorithm with equal CAP significantly decreases, and its minimum backscattering rate keeps unchanged. This can be explained by the increase in the required rate of the AD, which results in a corresponding increase in the SINR of the AD, thereby reducing the backscattering signal of the BDs and making the transmission rate of the BDs with high RC lower. This reason can also explain why the rate of the proposed algorithm is reduced. Besides, one should pay special attention to the fact that the gap between the maximum and minimum rates of the proposed algorithm is always much smaller than that of the algorithm with equal CAP, which exposes that the proposed algorithm has better resource usage fairness. The

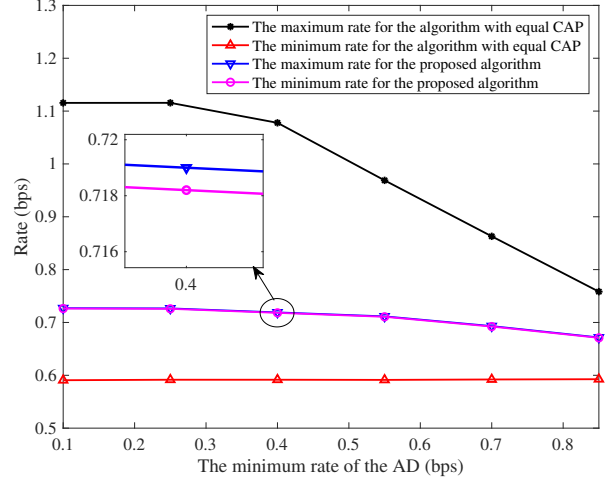


Fig. 6. Rate versus the minimum rate of the AD.

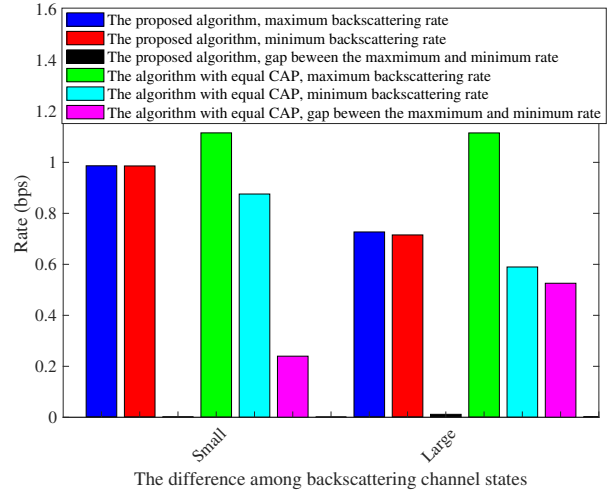


Fig. 7. Rate versus the different backscattering channel state.

reason is that the algorithm with equal CAP is mainly aimed at access fairness, which ignores the difference of channels between different BDs, resulting in the degradation of system performance.

To further prove the fairness of the proposed algorithm in terms of coping with channel differences, Fig. 7 presents the transmission rate versus the different backscattering channel states. When the channel difference is small, the rate gap of both algorithms is relatively small, and even the rate difference of the proposed algorithm is close to zero. When the channel difference becomes large, the rate gap of both algorithms increases, especially for the algorithm with equal CAP. It can be asserted that the proposed algorithm is better in guaranteeing the rate fairness regardless of the small or large channel differences, which is in contrast to the algorithm with equal CAP.

V. CONCLUSIONS

This paper investigates and analyzes the hybrid active and passive multiple access, where random access is considered for

$$P_m \geq \max \left\{ \frac{\Phi_n^{-1}(P_n^C)}{(1 - \alpha_n)|h_{m,n}^f|^2}, \frac{(2^{\bar{R}_n^{\min}} - 1) \sigma_w^2}{\text{Tr}(\mathbf{H}_m^d \mathbf{V}_{m\&n}) - (2^{\bar{R}_n^{\min}} - 1) \text{Tr}(\mathbf{H}_n^b \mathbf{V}_{m\&n}) \alpha_n |h_{m,n}^f|^2} \right\}. \quad (28)$$

multiple BDs. Specifically, a slotted ALOHA-based protocol is introduced to overcome the high overhead problem of traditional multi-access protocols in dealing with massive devices, and an optimization problem for rate fairness is formulated. Then, we transform the objective function with the max-min form into an equivalent linear one by using a slack variable, and decompose the resulting problem into three sub-problems. Next, a BCD-based algorithm with the penalty method, LP, and SCA is proposed to obtain the sub-optimal solutions. Simulation results demonstrate that the proposed algorithms outperform benchmark algorithms in terms of transmission performance and fairness.

APPENDIX A PROOF OF (21a) AND (21b)

It is easy to prove the objective function of problem (20) as a monotonically increasing function with respect to P_m and α_n , respectively. Therefore, we can assert that, regardless of which TA is selected, the optimal transmit power of this TA is $P_m^* = P_m^{\max}$. Besides, according to \bar{C}_3 and \bar{C}_4 , we have the lower bound for P_m , which is expressed as (28). Then, let $\alpha_n = 0$, which yields the minimum required transmit power of the AD when the harvested energy of the BD exactly compensate for its circuit power and no information is backscattered. Thus, we can obtain

$$P_{m\&n}^{\min} = \max \left\{ \frac{\Phi_n^{-1}(P_n^C)}{|h_{m,n}^f|^2}, \frac{(2^{\bar{R}_n^{\min}} - 1) \sigma_w^2}{\text{Tr}(\mathbf{H}_m^d \mathbf{V}_{m\&n})} \right\}. \quad (29)$$

On the other hand, according to \bar{C}_3 , \bar{C}_4 , and C_5 , we have

$$0 \leq \alpha_n \leq \begin{cases} \frac{\text{Tr}(\mathbf{H}_m^d \mathbf{V}_{m\&n}) P_m^{\max} - (2^{\bar{R}_n^{\min}} - 1) \sigma_w^2}{(2^{\bar{R}_n^{\min}} - 1) \text{Tr}(\mathbf{H}_n^b \mathbf{V}_{m\&n}) |h_{m,n}^f|^2 P_m^{\max}}, & \forall n. \\ 1 - \frac{\Phi_n^{-1}(P_n^C)}{P_m^{\max} |h_{m,n}^f|^2}. \end{cases} \quad (30)$$

Therefore, depending on its monotonicity, the optimal RC α_n^* can be obtained. In accordance with the above conclusions, the proof is complete.

REFERENCES

- [1] M. Vaezi *et al.*, "Cellular, wide-area, and non-terrestrial IoT: A survey on 5G advances and the road toward 6G," *IEEE Commun. Surveys Tuts.*, vol. 24, no. 2, pp. 1117–1174, 2nd Quart. 2022.
- [2] Y. Liu *et al.*, "Rethinking sustainable sensing in agricultural Internet of Things: From power supply perspective," *IEEE Wireless Commun.*, 2022. doi: 10.1109/MWC.004.2100426.
- [3] M. Centenaro *et al.*, "A survey on technologies, standards and open challenges in satellite IoT," *IEEE Commun. Surveys Tuts.*, vol. 23, no. 3, pp. 1693–1720, 3rd Quart. 2021.
- [4] Y. Xu *et al.*, "Joint computation offloading and radio resource allocation in MEC-based wireless-powered backscatter communication networks," *IEEE Trans. Veh. Tech.*, vol. 70, no. 6, pp. 6200–6205, Jun. 2021.
- [5] J. -P. Niu and G. Y. Li, "An overview on backscatter communications," *J. Commun. Inf. Netw.*, vol. 4, no. 2, pp. 1–14, Jun. 2019.
- [6] N. Van Huynh *et al.*, "Ambient backscatter communications: A contemporary survey," *IEEE Commun. Surveys Tuts.*, vol. 20, no. 4, pp. 2889–2922, 4th Quart. 2018.
- [7] D. Darsena, "Noncoherent detection for ambient backscatter communications over OFDM signals," *IEEE Access*, vol. 7, pp. 159415–159425, Oct. 2019.
- [8] H. Zhang, and L. Fan, "Adaptive mode selection for backscatter assisted communication systems with opportunistic SIC," *IEEE Trans. Veh. Tech.*, vol. 69, no. 2, pp. 2327–2331, Feb. 2020.
- [9] L. Shi *et al.*, "Energy efficiency for RF-powered backscatter networks using HTT protocol," *IEEE Trans. Veh. Tech.*, vol. 69, no. 11, pp. 13932–13936, Nov. 2020.
- [10] B. Gu *et al.*, "Many a little makes a mickle: Probing backscattering energy recycling for backscatter communications," *IEEE Trans. Veh. Tech.*, 2022, doi: 10.1109/TVT.2022.3205888.
- [11] Y. Xu *et al.*, "Robust energy-efficient optimization for secure wireless-powered backscatter communications with a non-linear EH model," *IEEE Commun. Lett.*, vol. 25, no. 10, pp. 3209–3213, Oct. 2021.
- [12] Y. Zhang, B. Li, F. Gao and Z. Han, "A robust design for ultra reliable ambient backscatter communication systems," *IEEE Internet Things J.*, vol. 6, no. 5, pp. 8989–8999, Oct. 2019.
- [13] D. Li and Y.-C. Liang, "Price-based bandwidth allocation for backscatter communication with bandwidth constraints," *IEEE Trans. Wireless Commun.*, vol. 18, no. 11, pp. 5170–5180, Nov., 2019.
- [14] D. Li, "Capacity of backscatter communication with frequency shift in Rician fading channels," *IEEE Wireless Commun. Lett.*, vol. 8, no. 6, pp. 1639–1643, Dec. 2019.
- [15] P. Zhang *et al.*, "Enabling practical backscatter communication for onbody sensors," in *Proc. ACM SIGCOMM*, pp. 370–383, Aug. 2016.
- [16] D. Li, "Two birds with one stone: Exploiting decode-and-forward relaying for opportunistic ambient backscattering," *IEEE Trans. Commun.*, vol. 68, no. 3, pp. 1405–1416, Mar. 2020.
- [17] D. Li, "Hybrid active and passive antenna selection for backscatter-assisted MISO systems," *IEEE Trans. Commun.*, vol. 68, no. 11, pp. 7258–7269, Nov. 2020.
- [18] Y. Ye *et al.*, "Delay minimization in wireless powered mobile edge computing with hybrid BackCom and AT," *IEEE Wireless Commun. Lett.*, vol. 10, no. 7, pp. 1532–1536, Jul. 2021.
- [19] X. Kang, Y. -C. Liang and J. Yang, "Riding on the primary: A new spectrum sharing paradigm for wireless-powered IoT devices," *IEEE Trans. Wireless Commun.*, vol. 17, no. 9, pp. 6335–6347, Sept. 2018.
- [20] D. Li, "Backscatter communication via harvest-then-transmit relaying," *IEEE Trans. Veh. Tech.*, vol. 69, no. 6, pp. 6843–6847, Jun. 2020.
- [21] D. Li, "Backscatter communication powered by selective relaying," *IEEE Trans. Veh. Tech.*, vol. 69, no. 11, pp. 14037–14042, Nov. 2020.
- [22] S. Han, Y. -C. Liang and G. Sun, "The design and optimization of random code assisted multi-BD symbiotic radio system," *IEEE Trans. Wireless Commun.*, vol. 20, no. 8, pp. 5159–5170, Aug. 2021.
- [23] H.-H. Choi and W. Shin, "Slotted ALOHA for wireless powered communication networks," *IEEE Access*, vol. 6, pp. 53342–53355, Sept. 2018.
- [24] S. A. Teges *et al.*, "Slotted ALOHA with NOMA for the next generation IoT," *IEEE Trans. Commun.*, vol. 68, no. 10, pp. 6289–6301, Oct. 2020.
- [25] Z. Hadzi-Velkov, S. Pejovski, N. Zlatanov and R. Schober, "Proportional fairness in ALOHA networks with RF energy harvesting," *IEEE Wireless Commun. Lett.*, vol. 8, no. 1, pp. 277–280, Feb. 2019.
- [26] S. Wang, M. Xia, K. Huang and Y. -C. Wu, "Wirelessly powered two-way communication with nonlinear energy harvesting model: Rate regions under fixed and mobile relay," *IEEE Trans. Wireless Commun.*, vol. 16, no. 12, pp. 8190–8204, Dec. 2017.
- [27] D. Xu *et al.*, "Resource allocation for IRS-assisted full-duplex cognitive radio systems," *IEEE Trans. Commun.*, vol. 68, no. 12, pp. 7376–7394, Dec. 2020.
- [28] K. Yang, T. Jiang, Y. Shi, and Z. Ding, "Federated learning via over-the-air computation," *IEEE Trans. Wireless Commun.*, vol. 19, no. 3, pp. 2022–2035, Mar. 2020.
- [29] X. Mu, Y. Liu, L. Guo, J. Lin, and R. Schober, "Simultaneously transmitting and reflecting (STAR) RIS aided wireless communications," *IEEE Trans. Wireless Commun.*, vol. 21, no. 5, pp. 3083–3098, May 2022.
- [30] S. Boyd and L. Vandenberghe, *Convex Optimization*. Cambridge, U.K.: Cambridge Univ. Press, 2004.
- [31] M. Grant and S. Boyd. (2008). *CVX: Matlab Software for Disciplined Convex Programming*. [Online]. Available: <http://cvxr.com/cvx>.